Classical computation of decoherence dynamics in continuous variable systems

To cite this article: Heekyung Han and Paul Brumer 2007 *J. Phys. B: At. Mol. Opt. Phys.* **40** S209

IOP Publishing Journal of Physics B: Atomic, Molecular and Optical Physics

J. Phys. B: At. Mol. Opt. Phys. **40** (2007) S209–S220 doi:10.1088/0953-4075/40/9/S13

Classical computation of decoherence dynamics in continuous variable systems

Heekyung Han and Paul Brumer

Chemical Physics Theory Group, Department of Chemistry and Center for Quantum Information and Quantum Control, University of Toronto, Toronto, Ontario, M5S 3H6, Canada

E-mail: hanh@chem.queensu.ca and pbrumer@chem.utoronto.ca

Received 18 December 2006, in final form 23 January 2007
Published 18 April 2007
Online at stacks.iop.org/JPhysB/40/S209

Abstract

The utility of classical mechanics to compute the dynamics of decoherence in continuous variable systems, as defined by the time dependence of the system purity, is examined. Its accuracy, in the semiclassical domain, is shown to depend on the nature of the coupling potentials and, less so, on the initial conditions. For a large range of cases, agreement between quantum and classical computations in small systems is shown to be excellent.

1. Introduction

Decoherence is the loss of coherence of a quantum system caused by ignoring (i.e., tracing over) degrees of freedom to which the system is coupled and which are regarded as of no interest. The latter is termed the bath, although it need not be larger than one degree of freedom. This journal volume is dedicated to aspects of decoherence and its control. Here we provide a contribution designed to explore the time evolution of decoherence (which we term the 'dynamics of decoherence') and to display the utility of classical mechanics as a simplifying tool to calculate it in continuous variable systems. It is motivated by interest in quantum control [1] in molecular environments, normally condensed phases. Typically, such situations are in the semiclassical, rather than fully quantal, regime.

For the past few decades, there has been considerable interest in understanding the nature of decoherence, both due to its role in bridging quantum and classical mechanics [2] and in its role as an obstacle in areas that exploit quantum coherence. The latter includes both quantum information and computation [3], as well as quantum control of atomic and molecular processes [1], where decoherence destroys the quantum coherence necessary for the processes of interest. Consequently, the need to protect quantum systems from deleterious decoherence effects has resulted in many approaches, several of which are discussed in that volume. Samples of earlier work include proposals in quantum computation (e.g. [4, 5]) and quantum control (e.g. [6]), and in selective suppression of decoherence via environmental engineering (e.g. [7–10]).

In the areas mentioned above, it is important to characterize the nature of decoherence. Despite significant work done on decoherence, particularly in studies of the emergence of the classical behaviour in the quantum world [2], not much attention has been paid to one interesting feature: the comparison between decoherence dynamics examined quantum mechanically and classically. Our focus here is on quantitative quantum–classical correspondence (QCC) in descriptions of decoherence dynamics, and upon the utility of classical mechanics as a tool in computing decoherence dynamics in continuous variable systems. Below, we use these two concepts interchangeably.

The idea of using classical dynamics to compute decoherence in such systems may seem odd, since the latter is purported to be a purely quantum property. However, according to the formal Liouville theory of QCC [11, 12], one can draw a strict analogy between quantum and classical dynamics in Hilbert space. In parallel with the nonunitarity and decoherence seen in the quantum reduced dynamics projected onto a smaller Hilbert subspace, we can expect that the classical Liouville dynamics projected onto a smaller subspace should also display the corresponding nonunitarity and classical decoherence. Using this motivation, Gong and Brumer [13] considered a direct classical computation of quantum decoherence dynamics using the purity [14] as the predominant measure [13, 15]. In particular, assuming that a contribution of N independent harmonic bath to the system-bath coupling potential is $\sum_{j=1}^{N} C_j q_j$ where q_j is a position variable of jth bath mode, analytical studies applying a second-order perturbative treatment showed the following : (i) excellent QCC in early-time decoherence dynamics exists if the system–bath coupling depends only linearly or quadratically on the system coordinates. This correspondence was found good for any initial state, regardless of $\hbar$, and irrespective of the system potential. (ii) Even in the case of highly nonlinear coupling, as long as the initial reduced density matrix in the position representation decays fast enough with relative distance of two positions, QCC would still be good. (iii) Otherwise, the correspondence can be poor. Since the second-order perturbative treatment is most reliable at short times and for weak decoherence (weak coupling strength), it is useful to examine this issue for longer times and for stronger coupling. This study, an extension of the numerical work in [15], is carried out below.

As a useful example we consider two interacting quartic oscillators, with the oscillator of interest denoted the 'system', S_1, and the other oscillator is the 'bath', denoted S_2. We demonstrate the dependence of QCC in the decoherence dynamics of S_1 on initial states of S_1, coupling potentials, and initial energies of the system. Initial states of S_1 discussed below include a single well-localized Gaussian state and a superposed two-Gaussian state (cat state). The coupling potential is chosen to be either biquadratic both in the coordinates of S_1 and S_2, which leads to regular or chaotic dynamics depending on the coupling strength, or more highly nonlinear coupling in the coordinate of S_1. Also examined is the effect of decreasing the initial system energies so as to approach the more quantum regime.

Our results both considerably extend as well as support the predictions of the earlier results [13, 15] on the QCC in the early time decoherence dynamics. Specifically, good QCC in decoherence dynamics is found not only for short times but also for long times in the following conditions: when the coupling is quadratic, when initial states are well localized, and when the initial energy is in the semiclassical limit. Results can also be good for initial delocalized cat states. Similarly, the perturbative result that highly nonlinear coupling potentials should destroy QCC are also verified numerically. Further, specific quantum effects, that become more evident at smaller $\hbar$, are seen to reduce quantum–classical agreement to short times, although the falloff rate of the decoherence is still well predicted classically for the cases examined.

This paper is organized as follows. Section 2 gives a general description for two interacting subsystems and then introduces the classical analogue of the quantum purity as a quantum decoherence measure. In section 3 several cases in the coupled-oscillator model systems are introduced, and a detailed numerical approach is presented. Then, in section 4, quantum and classical decoherence dynamics for these cases are investigated numerically by means of the purity. Concluding remarks comprise section 5.

2. Formulation

Consider a continuous variable system composed of two interacting subsystems S_1 and S_2, with the time-independent Hamiltonian:

$$H(Q, P, q, p) = H_{\mathrm{S}}(Q, P) + H_{\mathrm{B}}(q, p) + V_{\mathrm{SB}}(Q, q). \tag{1}$$

Here S_1 is the system of interest (denoted by the subscript S) and S_2 is the bath (denoted by the subscript B). The Hamiltonians of S_1 and S_2 are given by $H_{\mathrm{S}}(Q, P) = P^2/2 + V_{\mathrm{S}}(Q)$, $H_{\mathrm{B}}(q, p) = p^2/2 + V_{\mathrm{B}}(q)$ with (Q, P) and (q, p) being pairs of dimensionless phase-space conjugate variables. The potential $V_{\mathrm{SB}}(Q, q)$ couples the two subsystems. The focus is on the one degree of freedom for each subsystem, but it is straightforward to extend the discussion to additional degrees of freedom.

The classical phase space distribution function and the quantum phase space distribution function (here chosen as the Wigner function) are denoted by $\rho^c(Q, P, q, p, t)$ and $\rho^q(Q, P, q, p, t)$, respectively. Their time evolution equations are given by

$$\frac{\partial \rho^c}{\partial t} = \{H, \rho^c\}_P, \tag{2}$$

$$\frac{\partial \rho^q}{\partial t} = \{H, \rho^q\}_M, \tag{3}$$

where $\{\cdot\}_P$ and $\{\cdot\}_M$ denote the classical Poisson bracket and the quantum Moyal bracket [16, 11], respectively. Since one is often interested in only the dynamics of the subsystem S_1, we define, by tracing over S_2, the classical and quantum reduced distribution functions as

$$\tilde{\rho}_c(Q, P, t) \equiv \int \rho^c \, \mathrm{d}q \, \mathrm{d}p, \tag{4}$$

$$\tilde{\rho}_q(Q, P, t) \equiv \int \rho^q \, \mathrm{d}q \, \mathrm{d}p. \tag{5}$$

The purity, ς, which measures the decoherence of the S_1 system, or the entanglement of S_1 and S_2 is

$$\varsigma_q(t) = 2\pi\hbar \int \tilde{\rho}_q^2(Q, P, t) \, \mathrm{d}Q \, \mathrm{d}P, \tag{6}$$

where $\hbar$ is Planck's constant. The analogous classical purity ς_c can then be defined as

$$\varsigma_c(t) \equiv 2\pi\hbar \int \tilde{\rho}_c^2(Q, P, t) \, \mathrm{d}Q \, \mathrm{d}P. \tag{7}$$

In this paper the focus is on the time-dependent purity to examine quantum-classical correspondence in decoherence dynamics. Another more detailed, albeit representation dependent, measure of decoherence is the decay of off-diagonal reduced density matrix elements. Further studies on the QCC in terms of the reduced density matrix element in the position and energy representations are provided in [17].

3. Model and calculation method

3.1. Potentials

To examine QCC and the utility of classical computations of decoherence, we consider coupled-oscillator model systems. Here $V_S(Q)$ and $V_B(q)$ are chosen not to have simple harmonic terms, so that any observed agreement between classical and quantum behaviour cannot be ascribed to the similarity between classical and quantum harmonic oscillator dynamics. In particular, they are given by

$$V_S(Q) = \beta Q^4/4, \tag{8}$$

$$V_B(q) = \beta q^4/4 \tag{9}$$

with $\beta = 0.01$. Further, two different types of nonlinear coupling potentials are considered. One is quadratic in both Q and q, i.e., $V_{SB} = \alpha Q^2 q^2/2$. The resultant coupled oscillator is the well-known quartic oscillator model [18] whose dynamics can be strongly chaotic or integrable depending on the value of α. Specifically, two cases are examined, $\alpha = 1.0$ in the chaotic domain and $\alpha = 0.03$ in the integrable regime. The other potential used is a model highly nonlinear coupling case with $V_{SB} = \sin^2(10Q)q^2$.

3.2. Initial states: localized states and delocalized states

To compare decoherence dynamics using quantum and classical dynamics, we choose the initial quantum and classical distributions to be identical. This is the case even when the initial Wigner distribution has negative components, as discussed below.

In order to focus on decoherence produced during the interaction of the two subsystems, we choose an initial state that is a separable product of a system and a bath ρ is used. The same initial distribution is used for subsequent classical or quantum propagation, as described below. For simplicity we focus on how the initial states of S_1, rather than those of S_2, influence decoherence dynamics. In particular, we choose a well-localized single Gaussian state for the initial condition of S_2, but vary the degree of localization of the initial state of S_1. Specifically, the two different kinds of initial conditions of S_1 are examined, a well-localized single Gaussian, and a two well-separated Gaussians, a cat state. Wavefunctions for the case of an initial state that is a single Gaussian in both S_1 and S_2 are given by

$$\psi_S^0(Q) = \psi^G_{(Q_0,P_0)} \tag{10}$$

$$\equiv \left(\frac{1}{2\pi\sigma_Q^2}\right)^{1/4} \exp\left[-\frac{(Q-Q_0)^2}{4\sigma_Q^2} + \frac{\mathrm{i}P_0Q}{\hbar}\right], \tag{11}$$

$$\psi_B^0(q) = \left(\frac{1}{2\pi\sigma_q^2}\right)^{1/4} \exp\left[-\frac{(q-q_0)^2}{4\sigma_q^2} + \frac{\mathrm{i}p_0q}{\hbar}\right]. \tag{12}$$

Here $\psi^G_{(Q_0,P_0)}$ denotes a Gaussian wavepacket centred at Q_0 with a width δ_Q, moving with an initial momentum P_0. The initial total wavefunction $\psi^0(Q,q)$ is then given by

$$\psi^0(Q,q) = \psi_S^0(Q)\psi_B^0(q). \tag{13}$$

The corresponding initial density distribution functions for the two subsystems are obtained as a Wigner transform of $|\psi^0\rangle\psi^0$:

$$\tilde{\rho}_{\mathrm{S}}^{0}(Q,P) = \rho^{G}_{(Q_0,P_0)}(Q,P) \tag{14}$$

$$= \frac{1}{\pi\hbar}\exp\left[-\frac{(Q-Q_0)^2}{2\sigma_Q^2} - \frac{2\sigma_Q^2(P-P_0)^2}{\hbar^2}\right], \tag{15}$$

$$\tilde{\rho}_{\mathrm{B}}^{0}(q,p) = \frac{1}{\pi\hbar}\exp\left[-\frac{(q-q_0)^2}{2\sigma_q^2} - \frac{2\sigma_q^2(p-p_0)^2}{\hbar^2}\right], \tag{16}$$

$$\tilde{\rho}^{0}(Q,P,q,p) = \tilde{\rho}_{\mathrm{S}}^{0}(Q,P)\tilde{\rho}_{\mathrm{B}}^{0}(q,p). \tag{17}$$

Note that this initial distribution is positive everywhere, and is hence classical. However, its subsequent quantum evolution does not remain classical, introducing negative components in the Wigner distribution.

To investigate the effects of nonclassicality of the initial state, an initially superposed state of two Gaussian wavepackets for S_1, is also considered. This is given by

$$\psi_{\mathrm{S}}^{0}(Q) = N\left[\psi^{G}_{(Q_0,P_0)}(Q) + \psi^{G}_{(0,0)}(Q)\right], \tag{18}$$

with a normalization constant N, and a single Gaussian, for the initial wavefunction of S_2, given by equation (12). Note that here the initial S_1 state is composed of two Gaussians, one centred at (Q_0, P_0) and the other centred at $(0, 0)$. The corresponding initial density distribution function of S_1 is then

$$\tilde{\rho}_{\mathrm{S}}^{0}(Q,P) = N^2\left[\rho^{G}_{(Q_0,P_0)}(Q,P) + \rho^{G}_{(0,0)}(Q,P) + 2\rho^{\mathrm{INT}}(Q,P)\right], \tag{19}$$

where

$$\rho^{\mathrm{INT}}(Q,P) = \exp\left[-\frac{1}{2\sigma_Q^2}(Q-Q_0/2)^2 - \frac{2\sigma_Q^2}{\hbar^2}(P-P_0/2)^2\right]$$
$$\times\cos\left[-\frac{P_0Q}{\hbar} - \frac{Q_0P}{\hbar} - \frac{P_0Q_0}{2\hbar}\right]. \tag{20}$$

Thus, the initial density distribution for S_1 consists of three contributions, two of which correspond to the separate packets, and a third that is an interference term which takes on positive and negative values. Note that now this initial distribution as the total initial distribution in equation (17) is not positive everywhere, and is hence nonclassical. Classical propagation of such nonclassical distributions is discussed below.

We choose the dimensionless effective Planck constant as $\hbar = 0.005$ throughout, consistent with our interest in the semiclassical regime. For $S_1, \sigma_Q = \sigma_P = \sqrt{\hbar/2}$. For $S_2, \sigma_q = \sigma_p = \sqrt{\hbar/2}$. For the first quartic oscillator system $Q_0 = 0.4$, $P_0 = 0.5$, $q_0 = 0.6$, with p_0 chosen so as to make the energy equal to 0.24. For the second highly nonlinear system, $Q_0 = 0$, $P_0 = 0.5$, $q_0 = 0$ with energy 0.24.

Finally, the effect of decreasing the initial energy of the system on the QCC in the quartic oscillator system is studied using $Q_0 = 0.4/\sqrt{r}$, $P_0 = 0.5/\sqrt{r}$ and $q_0 = 0.6/\sqrt{r}$, with p_0 determined by fixing the energy at $0.24/r$, with a scaling factor r varying from 1, to 50, to 200.

3.3. Numerical methods

This subsection provides the numerical details related to obtaining the purity in the quantum and classical cases. For the quantum system, the total wavefunction, $\psi(Q, q, t)$ evolves under

the Schrödinger equation using the fast Fourier transform and split-operator method [19], and $\tilde{\rho}_q(Q_1, Q_2, t)$ is obtained as

$$\tilde{\rho}_q(Q_1, Q_2, t) = \int \mathrm{d}q\, \psi(Q_1, q, t)\psi^*(Q_2, q, t). \tag{21}$$

The purity is then given by

$$\begin{aligned}\varsigma_q(t) &= \int \langle Q_1|\hat{\tilde{\rho}}^2|Q_1\rangle \,\mathrm{d}Q_1 \\ &= \int \langle Q_1|\hat{\tilde{\rho}}|Q_2\rangle\langle Q_2|\hat{\tilde{\rho}}|Q_1\rangle \,\mathrm{d}Q_1\,\mathrm{d}Q_2 \\ &= \int |\tilde{\rho}_q(Q_1, Q_2, t)|^2 \,\mathrm{d}Q_1\,\mathrm{d}Q_2. \end{aligned} \tag{22}$$

Consider now the case of classical propagation. Here the classical trajectories evolve via Hamilton's equations from initial sets of (Q, P, q, p) that are distributed according to the initial quantum Wigner function, by combining the Monte Carlo sampling from the initial distribution and fourth-order Runge–Kutta integration. At the particular time t of interest, $\tilde{\rho}_c(Q, P, t)$ is obtained by simply counting the number of trajectories inside a bin located at Q to $Q + \Delta Q$, P to $P + \Delta P$ and ignoring (q, p). Purity is then computed via equation (7). Note two numerical features. First, an enormous gain in numerical efficiency can be obtained by *ignoring* the (q, p) variables in the construction of $\tilde{\rho}_c(Q, P, t)$. This is equivalent to tracing over the q, p variables. Second, in cases where the initial $\rho_c(Q, P, q, p; t)$ is initiated as the Wigner representation of a non-classical state, there are values of Q, P, q, p for which the $\rho_c(Q, P, q, p; 0)$ are negative. These are dealt with by weighting the propagated trajectory at time t by the associated negative weight.

4. Results

This section presents computational results for quantum and classical decoherence dynamics in terms of the purity for a system of two quartic oscillators subjected to two different types of coupling potentials with various initial conditions for the subsystem S_1.

It is noteworthy that there are two aspects of studying quantum decoherence dynamics of interest. One is comparing quantum decoherence dynamics with its classical counterpart to examine QCC in decoherence dynamics and to understand the utility of classical computations, which was the original motivation for this study. The other is examining quantum decoherence dynamics in itself; for example, determining the quantum decoherence time after which quantum coherence is lost, and investigating how the decoherence rate depends on the nature of the coupling potentials and the initial conditions. Early studies of the decoherence in a system coupled to an environment with many degrees of freedom showed that the decoherence rate tends to be determined by the system dynamics itself [20] after the initial onset of decoherence which is dependent on the strength and nature of the coupling with the environment [21] and on the form of the initial state [22, 23]. Since our bath has only one degree of freedom, direct comparisons may not be possible but some similar relevant characteristics may be found.

4.1. Initially localized states

4.1.1. $V_{\mathrm{SB}}(Q, q) = \alpha q^2 q^2/2$. Consider first the quartic oscillator model with localized initial Gaussian states, for both integrable and chaotic cases. Preliminary comparisons of quantum and classical linear entropies for these cases were studied in [15], and showed excellent

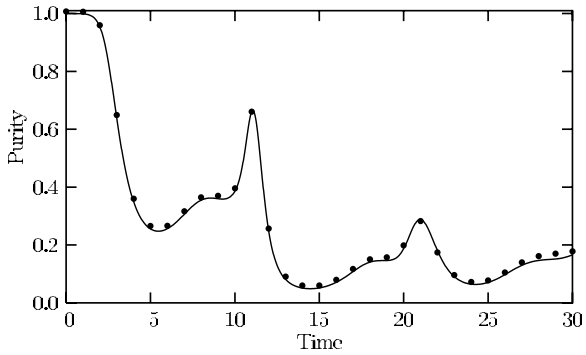

Figure 1. Comparison between $\varsigma_q(t)$ (solid line) and $\varsigma_c(t)$ (discrete filled circular points) for the quartic oscillator model in the case of integrable dynamics ($\alpha = 0.03$). $\sigma_Q = \sigma_P = \sqrt{\hbar/2}$, $Q_0 = 0.4$, $P_0 = 0.5$, q_0=0.6 with initial state energy of 0.24. All variables are in dimensionless units.

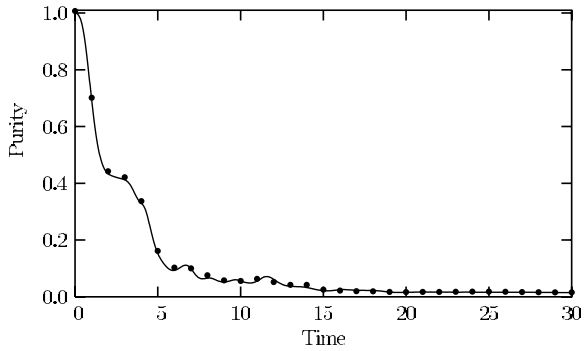

Figure 2. As in figure 1 but for strongly chaotic dynamics ($\alpha = 1.0$).

agreement. To obtain the accurate classical results of $\mathrm{Tr}_1(\hat{\tilde{\rho}}^2)$, that paper integrated the product of two initial states, $\rho^c(Q, P, q, p, 0)\rho^c(Q'', P'', q'', p'', 0)$, where (Q'', P'', q'', p'') is the phase-space location of the trajectory at $t = 0$ if the classical trajectory is propagated backwards from $(Q(t), P(t), q', p')$, and $(Q(t), P(t), q(t), p(t))$ is the phase-space location of the trajectory from (Q, P, q, p) at $t = 0$ (for details, see equation (27) in [15]). The method used here, and described above, is far more efficient.

Figure 1 shows the quantum and classical purities for the integrable case. The purities $\varsigma_q(t)$ and $\varsigma_c(t)$ are in excellent agreement with one another over the entire time, and relax towards zero through large-amplitude oscillations. The observed oscillatory behaviour indicates that S_1 recovers coherence in some periodic way. To clarify the possible relation between the periodic motion of the purity and that of the S_1, we calculated the expectation value of Q (denoted as $\langle Q\rangle$) and the variance of Q (denoted as $\langle \Delta Q^2\rangle (\equiv \langle Q^2\rangle - \langle Q\rangle^2)$) and found that the period of the purity is roughly half of the period of the S_1 oscillation (not shown here). More interestingly, the local maxima (minima) in the purity occur when the $\langle \Delta Q^2\rangle$ has local maxima (minima). This observation is consistent with that in [24] which shows strong correlation between maxima (minima) of the linear entropy and the smallest (largest) distance from the classical phase-space border in the N-atom Jaynes–Cummings model.

For the chaotic case, figure 2 shows the purities versus time. (Note that the chaoticity in our system is brought about by the strong coupling between the two subsystems. Thus, it

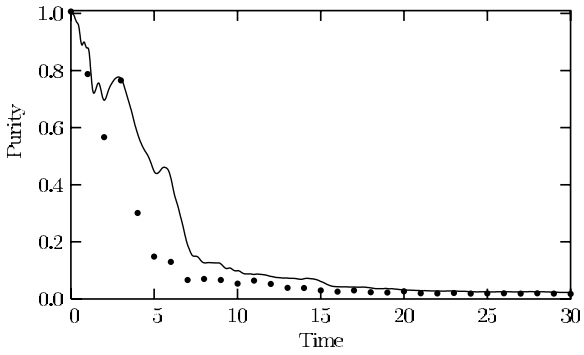

Figure 3. A comparison between $\varsigma_q(t)$ (solid line) and $\varsigma_c(t)$ (points) for the highly nonlinear coupling potential case $V_{\rm SB}(Q,q) = \sin^2(10Q)q^2$ with $\sigma_Q = \sigma_P = \sqrt{\hbar/2}$. All variables are in dimensionless units.

is different from [23, 25] where a classically chaotic system coupled to the environment is shown to decohere faster than the corresponding integrable system.) Figure 2 demonstrates that even for the chaotic case, quantum and classical purities are in excellent agreement. For the chaotic case the purity shows not only a faster decay at early times but also a much faster relaxation towards a plateau with smaller-amplitude oscillations at long times, than does the integrable case (figure 1). This larger coupling strength in the chaotic case leads to a more rapid diagonalization of the reduced density matrix when compared to the integrable case (not shown here, see [17]). This is consistent with an observation in [26] that the case of larger coupling between two subsystems results in more rapidly diagonalized reduced density matrices. Good QCC observed in decoherence dynamics for the above system in the integrable and chaotic cases indicates that decoherence originates largely in the classical correlations of two subsystems that is produced during the dynamical evolution, and seems not to be associated strongly with intrinsic quantum effects such as interference [27, 28].

4.1.2. $V_{\rm SB}(Q,q) = \sin^2(10Q)q^2$. Consider now $V_{\rm SB}(Q,q) = \sin^2(10Q)q^2$ as an example of a highly nonlinear potential in Q, which is expected [15] to show poor agreement between quantum and classical decoherence dynamics. For this coupling potential, Gong and Brumer suggested, from their early-time perturbation result in [15], that there can be a substantial classical entropy production with negligible quantum decoherence, and confirmed their prediction numerically for a strongly squeezed wavepacket of S_1 in P with $\sigma_Q/25 = 25\sigma_P = \sqrt{\hbar/2}$ at early times up to $t = 4$. Here we examine the case with $\sigma_Q = \sigma_P = \sqrt{\hbar/2}$, i.e., the same uncertainty in both position and momentum. The quantum and the classical purities versus time are presented up to $t = 30$ in figure 3.

Additional studies indicated that the more delocalized the initial wavepacket, the poorer the quantum–classical correspondence, especially at early times. Careful comparisons suggest that the larger discrepancy between the quantum and classical purities with increasing degree of initial delocalization arises from the fact that the classical purity decays much faster at initial times for larger σ_Q, whereas the quantum counterpart is relatively insensitive to changes in the extent of delocalization. Thus, an initially highly localized wavepacket is expected to improve the agreement between quantum and classical decoherence dynamics even for this highly nonlinear coupling potential. Moreover, although Gong and Brumer argued that poor QCC at early times suggests similar behaviour at later times, this may not always be the case.

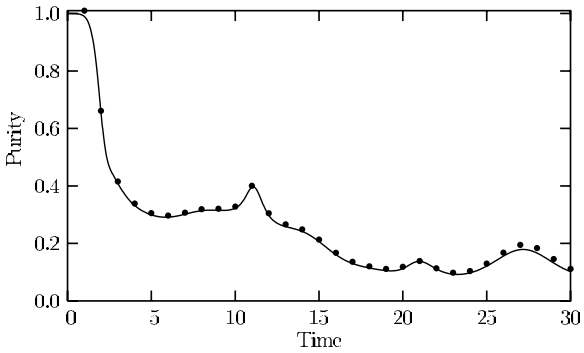

Figure 4. A comparison between $\varsigma_q(t)$ (solid line) and $\varsigma_c(t)$ (points) for an initial coherent and symmetrical superposition of two Gaussians which are well separated at (0.4, 0.5) and (0, 0) in phase space (Q, P) with width $\sigma_Q = \sigma_P = \sqrt{\hbar/2}$ for the quartic oscillator model in the case of integrable dynamics ($\alpha = 0.03$). All variables are in dimensionless units.

Figure 3 shows that after a substantial decay of purity, QCC in terms of purity seems to be recovered at $t = 17$. By this time, however, the absolute magnitude of the purity becomes quite small, suggesting the need for alternative comparative measures. In fact, other studies do indicate that, as time increases, both the quantum and classical reduced density matrices become quite diagonally dominant but with significant differences along the on-diagonal axis (not shown here, see [17]).

4.2. Initially superposed states

Consider now the case of two initially well-separated Gaussian state in S_1, namely, a Schrödinger 'cat' state, given by equation (18), using the quartic oscillator model with $\alpha = 0.03$. Note that the use of an initially cat state introduces nonclassical nature to the initial state of S_1, and thus this may lead to breakdown of the QCC that existed for an initially single Gaussian state, as seen in figure 1. Nonetheless, figure 4 shows excellent agreement between quantum and classical purities. Note that all initially superposed states need not produce good QCC in decoherence dynamics. Further studies, reported in [17], show that there can be significant differences in the QCC depending on the symmetry of the initially two separated Gaussians. In particular, when the system is initially symmetric in both the position and momentum coordinate, that is, the two Gaussian wavepackets are centred at (Q_0, P_0) and $(-Q_0, -P_0)$ in phase space (Q, P), the QCC in decoherence dynamics is poor. This is attributed to a parity conservation property which exists only in quantum dynamics [17].

4.3. Energy variations

The results above are in the semiclassical energy regime. Here we consider smaller initial energies to expose classical–quantum differences as the more quantum regime is accessed. Figure 5 shows results for the quartic oscillator model in the integrable ($\alpha = 0.03$) and chaotic ($\alpha = 1.0$) cases for three different energies. For simplicity, the initial condition is limited to the localized single Gaussian state with $\sigma_Q = \sigma_P = \sqrt{\hbar/2}$. A number of features are evident. Note first aspects of the quantum results, independent of a classical comparison. (Care must be taken in making a comparison between different quantum cases since each of the cases shown corresponds to a state with different energy, but also with different Q_0, P_0, q_0, p_0. However,

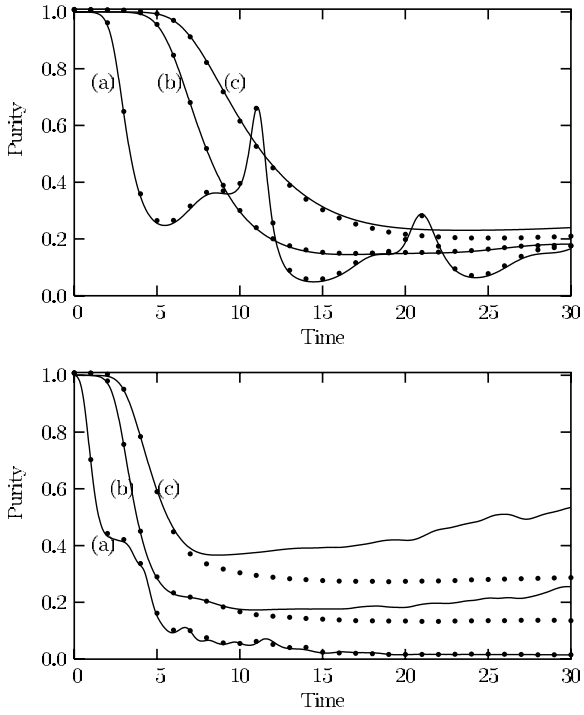

Figure 5. Effects of different initial energies on quantum–classical correspondence are shown by comparisons of $\varsigma_q(t)$ (solid line) and $\varsigma_c(t)$ (points); the top panel (bottom) corresponds to the quartic oscillator model in the case of integrable (chaotic) dynamics with $\alpha = 0.03$ ($\alpha = 1.0$). For all cases, $\sigma_Q = \sigma_P = \sqrt{\hbar/2}$. $Q_0 = 0.4/\sqrt{r}$, $P_0 = 0.5/\sqrt{r}$, $q_0 = 0.6/\sqrt{r}$ and p_0 is chosen so that the state energy is $0.24/r$; (a) $r = 1$, (b) $r = 50$ and (c) $r = 200$. All variables are in dimensionless units.

there are a number of interesting features.) First, the asymptotic value of the purity, which reflects $1/$(the number of orthogonal states available to S_1) increases with decreasing energy in both the chaotic case (lower panel), and in the integrable case (top panel), as expected. Surprisingly, however, the two lower energy states in the chaotic case show a minimum with no classical analogue, in the purity versus time at around $t = 10$. Further, the different states studied show longer initial regions of flat behaviour as the energy decreases. However, it is difficult to state, without further study, whether the latter feature is a characteristic that is solely dependent upon the state energy or whether it depends upon other attributes of the initial states.

Consider now the utility of the classical computation of the decoherence dynamics as a function of energy. First note that at short times agreement between the quantum and classical purities is excellent for all cases examined, irrespective of the magnitude of initial energies [13, 15]. Indeed, in all cases the classical mechanics adequately predicts the decay rates of the decoherence and, in the integrable case, the agreement is almost perfect at longer times as well. For sufficiently low energies, however, it would appear that this degree of agreement would diminish [27]. Second, as time increases, agreement between the quantum and classical purities worsens with decreasing energy, with the discrepancies becoming far more significant in the chaotic case (figure 5). This long time discrepancy is due to the number of available states at that energy. For example, numerical results show that the number of the quantum energy eigenstates available to S_1 is only 5 for case (c), while no such restriction applies in the

classical case. Hence the long time classical purity is seen to be a lower bound to the quantum purity. Further work is necessary to establish an *a priori* measure of the time scale over which the classical dynamics is expected to be a good approximation as a function of energy.

5. Conclusion

This paper has numerically demonstrated the utility of classical computations of quantum decoherence over all times for cases which were analytically predicted [13] to have good classical–quantum correspondence for decoherence over short times. Similarly, cases where perturbation theory predicted poor correspondence indeed showed significantly different quantum and classical behaviour. Studies of representation-dependent measures of decoherence such as the density in the coordinate and energy representation, to be reported elsewhere [17], also support these conclusions. Naturally, the numerical results are limited in scope, but nonetheless are encouraging as to the utility of classical computational methods for computing decoherence dynamics in the semiclassical regime. It also brings up the important issue of designing measures that truly distinguish between the decoherence and associated entanglement that exist in quantum mechanics, and the classical correlations that seem to often well mimic this dynamics as exposed using the purity measure.

There are various ways in which this work can be extended. One important direction would be to examine systems with large numbers of degrees of freedom, noting that our classical numerical method is much easier to extend to larger systems than are previous [15] approaches. Work in this direction is now in progress [29].

Acknowledgments

We thank Professor Jiangbin Gong, now at the University of Singapore, for discussions early in this work. We acknowledge financial support from the Natural Sciences and Engineering Research Council of Canada, and Photonics Research Ontario.

References

[1] Shapiro M and Brumer P 2003 *Principles of the Quantum Control of Molecular Processes* (Hoboken, NJ: Wiley-Interscience)
[2] Zurek W H 2003 *Rev. Mod. Phys.* **75** 715
Joos E, Zeh H-D, Kiefer C, Guilini D, Jupsch J and Stamatescu I-O 2003 *Decoherence and the Appearance of a Classical World in Quantum Theory* 2nd edn (Berlin: Springer) and references therein
[3] Nielsen M A and Chuang I L 2000 *Quantum Computation and Quantum Information* (Cambridge: Cambridge University Press)
[4] Shor P W 1995 *Phys. Rev.* A **52** 2493
Steane A M 1996 *Phys. Rev. Lett.* **77** 793
Knill E and Laflamme R 1997 *Phys. Rev.* A **55** 900
[5] Duan L-M and Guo G-C 1997 *Phys. Rev. Lett.* **79** 1953
Zanardi P and Rasetti M 1997 *Phys. Rev. Lett.* **79** 3306
Lidar D A, Chuang I L and Whaley K B 1998 *Phys. Rev. Lett.* **81** 2594
Wiseman H M and Milburn G J 1993 *Phys. Rev. Lett.* **70** 548
[6] Shapiro M and Brumer P 1989 *J. Chem. Phys.* **90** 6179
[7] Carvalho A P R, Millman P, de Mattos Filho R L and Davidovich L 2001 *Phys. Rev. Lett.* **86** 4988
[8] Poyatos J F, Cirac J I and Zoller P 1997 *Phys. Rev. Lett.* **77** 4728
[9] Myatt C J, King B E, Turchette Q A, Sackett C A, Kielpinski D, Itano W M, Monroe C and Wineland D J 2000 *Nature* **403** 269
[10] Shapiro M and Brumer P 2002 *Phys. Rev.* A **66** 052308

[11] Wilkie J and Brumer P 1997 *Phys. Rev.* A **55** 27
Wilkie J and Brumer P 1997 *Phys. Rev.* A **55** 43
[12] Brumer P and Gong J 2006 *Phys. Rev.* A **73** 052109
[13] Gong J and Brumer P 2003 *Phys. Rev. Lett.* **90** 050402
[14] Lichtner P C and Griffin J J 1976 *Phys. Rev. Lett.* **37** 1521
Zurek W H, Habib S and Paz J P 1993 *Phys. Rev. Lett.* **70** 1187
Nemes M C and deToledo Piza A F R 1986 *Physica* A **137** 367
Jiang X-P and Brumer P 1993 *Chem. Phys. Lett.* **208** 179
[15] Gong J and Brumer P 2003 *Phys. Rev.* A **68** 022101
[16] Moyal J E 1949 *Proc. Camb. Phil. Soc.* **45** 99
[17] Han H and Brumer P (in preparation)
[18] See, e.g. Eckhardt B, Hose G and Pollak E 1989 *Phys. Rev.* A **39** 3776
[19] Feit M D, Fleck J A and Steiger A 1982 *J. Comput. Phys.* **47** 412
[20] Zurek W H and Paz J P 1994 *Phys. Rev. Lett.* **72** 2508
[21] Paz J P, Habib S and Zurek W H 1993 *Phys. Rev.* D **47** 488
[22] Zurek W H 1982 *Phys. Rev.* D **26** 1862
[23] Zurek W H and Paz J P 1995 *Physica* D **83** 300
Zurek W H, Habib S and Paz J P 1993 *Phys. Rev. Lett.* **70** 1187
[24] Angelo R M, Furuya K, Nemes M C and Pellegrino G O 2001 *Phys. Rev.* A **64** 043801
[25] Pattanayak A K and Brumer P 1997 *Phys. Rev. Lett.* **79** 4131
Tameshtit A and Sipe J E 1993 *Phys. Rev.* A **47** 1967
[26] Lakshminarayan A 2001 *Phys. Rev.* E **64** 036207
[27] For related work at lower energies using an alternate approach see Angelo R M and Furuya K 2005 *Phys. Rev.* A **71** 042321
[28] Han H and Brumer P 2005 *J. Chem. Phys.* **122** 144316
[29] Elran Y, Kapral R and Brumer P (in preparation)